



HAL
open science

Kinetic and Fluid Dynamics Modeling of Methane/Hydrogen Jet Flames in Diluted Coflow

Alessio Frassoldati, Pratyush Sharma, Alberto Cuoci, Tiziano Faravelli, Eliseo
Ranzi

► **To cite this version:**

Alessio Frassoldati, Pratyush Sharma, Alberto Cuoci, Tiziano Faravelli, Eliseo Ranzi. Kinetic and Fluid Dynamics Modeling of Methane/Hydrogen Jet Flames in Diluted Coflow. Applied Thermal Engineering, 2009, 30 (4), pp.376. 10.1016/j.applthermaleng.2009.10.001 . hal-00593335

HAL Id: hal-00593335

<https://hal.science/hal-00593335>

Submitted on 14 May 2011

HAL is a multi-disciplinary open access archive for the deposit and dissemination of scientific research documents, whether they are published or not. The documents may come from teaching and research institutions in France or abroad, or from public or private research centers.

L'archive ouverte pluridisciplinaire **HAL**, est destinée au dépôt et à la diffusion de documents scientifiques de niveau recherche, publiés ou non, émanant des établissements d'enseignement et de recherche français ou étrangers, des laboratoires publics ou privés.

Accepted Manuscript

Kinetic and Fluid Dynamics Modeling of Methane/Hydrogen Jet Flames in Diluted Coflow

Alessio Frassoldati, Pratyush Sharma, Alberto Cuoci, Tiziano Faravelli, Eliseo Ranzi

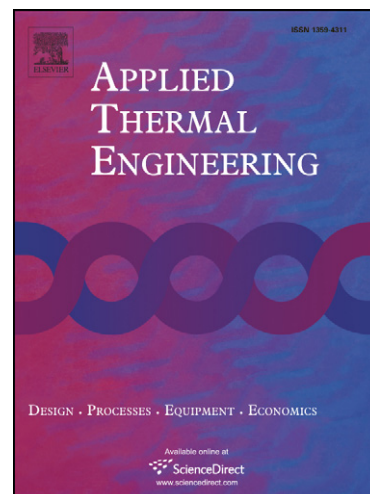
PII: S1359-4311(09)00292-0
DOI: [10.1016/j.applthermaleng.2009.10.001](https://doi.org/10.1016/j.applthermaleng.2009.10.001)
Reference: ATE 2897

To appear in: *Applied Thermal Engineering*

Received Date: 15 May 2009
Accepted Date: 1 October 2009

Please cite this article as: A. Frassoldati, P. Sharma, A. Cuoci, T. Faravelli, E. Ranzi, Kinetic and Fluid Dynamics Modeling of Methane/Hydrogen Jet Flames in Diluted Coflow, *Applied Thermal Engineering* (2009), doi: [10.1016/j.applthermaleng.2009.10.001](https://doi.org/10.1016/j.applthermaleng.2009.10.001)

This is a PDF file of an unedited manuscript that has been accepted for publication. As a service to our customers we are providing this early version of the manuscript. The manuscript will undergo copyediting, typesetting, and review of the resulting proof before it is published in its final form. Please note that during the production process errors may be discovered which could affect the content, and all legal disclaimers that apply to the journal pertain.



Kinetic and Fluid Dynamics Modeling of Methane/Hydrogen Jet Flames in Diluted Coflow

Alessio Frassoldati, Pratyush Sharma, Alberto Cuoci, Tiziano Faravelli and Eliseo Ranzi

Dipartimento di Chimica, Materiali e Ingegneria Chimica "G. Natta", Politecnico di Milano,
Piazza L. Da Vinci 32, 20133 Milano (Italy)

Corresponding author: alessio.frassoldati@polimi.it

Tel + 39 02 2399 3286

Fax + 39 02 7063 8173

Abbreviated Title: CFD and kinetic modeling of MILD combustion

Keywords: Combustion; NO_x prediction; Kinetics; Turbulence

Abstract

MILD combustion is a recent development in the combustion of hydrocarbon fuels which promises high efficiencies and low NO_x emissions. In this paper we analyze the mathematical and numerical modeling of a Jet in Hot coflow (JHC) burner, which is designed to emulate a moderate and intense low oxygen dilution (MILD) combustion regime [1]. This paper initially discusses the effects of several modeling strategies on the prediction of the JHC flame structure using the CFD code FLUENT 6.3.26. Effects of various turbulence models and their boundary conditions have been studied. Moreover, the detailed kinetic mechanism adopted in the CFD simulations is successfully validated in the conditions of interest using recent literature data [2] on the effect of nitrogen dilution on the flame speeds of several CH₄/H₂/air lean mixtures. One of the aims of this paper is also to describe a methodology for computing pollutant formation in steady turbulent flows to verify its applicability to the MILD combustion regime. CFD results are post-processed for calculating the NO_x using a numerical tool called Kinetic Post Processor (KPP). The modeling results agree with the experimental results [1] and support the proposed approach as a useful tool for optimizing the design of new burners also in the MILD combustion regime.

1. Introduction

The increasing energy demand and concern on the combustion-generated pollution force to seek for new combustion technologies which are more efficient and environmental friendly. MILD combustion is a technique which offers a possible solution to this problem. This technology is named differently like High Temperature Air Combustion (HiTAC) in Japan, MILD combustion in Italy and Flameless Combustion in Germany. The basic aspect of this combustion regime is that highly diluted and preheated air is mixed with fuel to form a more uniform combustion zone which gives better efficiency, higher radiation flux and low pollutants. In this regime combustion takes place in a more diluted fashion and thus temperature peaks, responsible for NO_x formation, can be avoided. Wunning and Wunning [3] showed flameless combustion technique as highly efficient and with Low NO_x emissions. They also showed that thermal NO_x which is a major source of NO_x formation in combustion systems can be reduced by reducing the peak temperature, which is one of the best outcomes of this combustion regime. Weber et al. [4] conducted experiments on semi industrial scale burner to study this combustion regime. The combustion chamber was operated close to well stirred reactor conditions and found to have a high and uniform radiative flux on chamber walls. Katsuki and Hasegawa [5] studied MILD combustion in a heat recirculating semi industrial furnace to find this technique as highly energy efficient and with significantly low NO_x emissions. De Joannon et al. [6] studied the applicability of existing reaction mechanisms to study MILD combustion technique. Although the concept of MILD combustion has been extensively investigated, mathematical modeling of flameless combustion regime has received less attention [7]. The modeling of this combustion regime needs specific attention. In fact it does not feature high-density gradients and complex turbulence–chemistry interaction processes, which are prominent in conventional turbulent jet flames. However, the conditions of uniform temperature distribution and low oxygen concentration lead to slower reaction rates and enhance the influence of molecular diffusion on flame characteristics, particularly when hydrogen is present in the fuel. These two effects, in particular, challenge the applicability of combustion models that assume fast chemistry and neglect the effects of differential diffusion [7].

Coelho and Peters [8] carried out numerical simulation on MILD combustion FLOX burner and showed that the steady flamelet library was unable to correctly describe the formation of NO. In fact, NO formation is a slow process, and therefore is sensitive to transient effects. On the contrary the unsteady flamelet model was able to predict the correct order of magnitude of NO emissions. Mancini et al [9] reported predictions of NO_x in large scale burner operated in

flameless mode. Kim et al. [10] used conditional moment closure (CMC) method to model flames experimentally measured by Dally et al. [1].

In this paper the effects of oxygen concentration in a hot diluted oxidant stream are investigated in the experimental condition of Dally et al. [1], who developed the JHC (Jet in Hot Coflow) burner to emulate the MILD combustion regime. Christo and Dally [7] successfully modeled this burner using the eddy dissipation concept (EDC) model to describe the turbulence-chemistry interactions and a detailed kinetic mechanism. The accuracy of the numerical solution was found to be highly sensitive to boundary conditions, especially turbulence quantities. The modeling results also demonstrated that conserved scalar-based models are inadequate for modeling the JHC flame. The EDC model, however, yielded reasonable results if used in conjunction with detailed mechanisms. The use of a skeletal kinetic mechanism to represent the chemistry was found to reduce the accuracy of the predictions [7]. The EDC model revealed to be capable of capturing flame liftoff, but was not accurate enough in predicting the flame liftoff distance [7]. In this paper we take advantage of the indications of Christo and Dally [7] and used the EDC to model turbulence-chemistry interactions using the detailed kinetic mechanism described in paragraph 2. The interest in the EDC model is further motivated by the possibility to couple CFD simulations and detailed kinetics with a reduced computational effort than more complex and CPU-intensive approaches. This advantage of the EDC model allows to solve larger problems, such as those associated with the complex geometries of industrial applications.

In this paper we refer to the JHC burner and initially discuss effects of different models and boundary conditions adopted in the CFD simulation. The best CFD flame results are post processed to calculate the NO_x formation using our numerical tool KPP. This numerical code has been already applied to the modeling of laboratory burners [11,12], industrial burners, combustors and furnaces [13,14, 15]. The final aim of this paper is to verify the applicability of this methodology to the MILD combustion regime.

2. Description of Detailed Chemical Kinetic Mechanism

A semi-detailed kinetic scheme able to describe the oxidation of gaseous and liquid hydrocarbon fuels, from methane up to diesel and jet fuels, has been developed and its main features have been already discussed in the literature [16,17,18].

Due to the hierarchical modularity of the mechanistic kinetic model, the combustion mechanism is based on a detailed sub-mechanism of C1-C4 species. The chemistry of nitrogen compounds is included in the mechanism and is discussed elsewhere [17,19]. The overall hydrocarbon and

NO_x kinetic scheme, are available on the web (<http://www.chem.polimi.it/CRECKModeling>).

The methane/CO/H₂ sub-mechanism is used in the CFD simulations. This scheme consists of 48 chemical species involved in ~600 reactions and is available upon request. The NO_x species are added to this mechanism when the KPP is used.

The ability of this mechanism to accurately describe the combustion of H₂, syngas and other fuel mixtures was already verified and discussed [20-22].

The mechanism is here further verified using recent laminar flame speed measurements [2].

Figure 1 shows a comparison between experimental measurements and model predictions. The agreement is very satisfactory and confirms the capability of the kinetic mechanism to capture the effect of hydrogen addition on flame speed. Moreover, the effect of nitrogen dilution (temperature) is also correctly described.

3. Burner Description and Computational Domain

Numerical simulations are performed to model the flame generated in the JHC burner developed and experimentally studied by Dally et al. [1].

The experimental burner shown consists of a central fuel jet (i.d. = 4.25 mm) and is surrounded coaxially by an annulus (i.d. = 82 mm) equipped with a secondary burner. The annulus contains the hot coflow flue gases produced by the secondary burner. The whole facility is placed inside a tunnel. Details on the geometry can be found in ref. [1].

The flames were simulated with the commercial CFD code FLUENT 6.3.26. A 2D steady-state simulation of the physical domain was considered due to the axial symmetry of the system.

Figure 2 shows the computational grid used to simulate the flames. It is a structured non uniform grid with about 35000 cells, designed to give high resolution in the flame region and close to the inlets and save computational efforts elsewhere. The grid-independency of the results was verified using a finer grid with a number of cells of ~140000. The grid domain is 400 mm in axial and 120 mm in radial direction from the jet exit. The mesh elements used are Quadrilateral. As suggested by the authors of the experimental activity the experimental data at 4 mm from jet exit are used as boundary profiles for the coflow inlet of the computational domain. Tab. 1 summarizes the assumed boundary conditions. This is non-confined flame, for this reason a pressure outlet condition is used (see Fig. 2) assuming ambient air conditions for the backflow. The simulations were performed with three different O₂ mass fraction profiles in the Coflow. The mean (approximate) O₂ mass fractions in Coflow profiles are 3%, 6% and 9%. Figure 3 shows

the relevant effect of the different amount of oxygen in the oxidizer. A flame lift off is visible and combustion occurs with weaker or higher intensity according to the oxygen content in the oxidizer stream.

4. Numerical modeling

The burner was modeled using several turbulence and radiation models to simulate the flames. Turbulence was modeled via the RANS approach, using the k - ε and the Reynolds Stress Model (RSM).

The Standard k - ε model is known for its shortcomings in predicting round jets. In particular, the standard k - ε model overpredicts the decay rate and the spreading rate of a round jet.

Modifications for the parameter $C_{\varepsilon 1}$ lead to a value of 1.60 for self-similar round jets [23].

Figure 4 shows the comparison between experimental measurements and model predictions along the axis of symmetry. Mixture fraction is used to describe the mixing between the fuel jet and the surrounding oxidizer and it is also a good indicator of the jet penetration. The RSM and the modified k - ε model perform very well while the standard k - ε model underpredicts the jet penetration. The k - ε model is used in all the simulations in order to avoid the additional computational expense of the Reynolds stress model, and to concentrate on the study of turbulence-chemistry interactions.

As already observed [7], the numerical solution is highly sensitive to the turbulence level at the inlets. In order to reduce the computational time and effort, it was decided not to simulate the complete (complex) geometry ahead of the coflow inlet, which contains a secondary burner and a perforated plate. For the fuel inlet, the turbulence level proposed in [7] is used. It is important to notice that the turbulence level at the coflow inlet boundary directly affects the value of the turbulent viscosity, which controls the turbulent diffusion. For this reason, the amount of oxygen which diffuses from the shroud air towards the flame is significantly affected by the boundary conditions.

Figure 5 shows the effect of different values used of the boundary condition of the turbulent kinetic energy. As expected, the lower the value of k is, the lower the diffusion of oxygen from the surrounding air to the flame region. Figure 6 shows the effect of the different k values on the O_2 radial profiles at two different axial locations ($z=30$ mm and $z=120$ mm). The comparison shows that a value of $k = 0.4\text{m}^2/\text{s}^2$, when used for simulating the flame resulted in good agreement with experimental measurements.

We used different radiation models (P1, Discrete ordinates (DO) [24] and Sandia model [25]). Although in this particular burner configuration the effect of thermal radiation is not particularly significant, especially in the first part of the flame, the best results were found using the DO model. The WSGGM (weighted sum of gray gas) model is used to calculate the total emissivity as a function of gas composition and temperature. Different models were used for the description of the turbulence/chemistry interactions. As already observed by Christo and Dally [7], using detailed chemical kinetics, rather than global or skeletal mechanisms improves the accuracy significantly. Differential diffusion is always accounted for, as it is known to have a strong influence on predictions because of the high hydrogen content in the fuel [7]. A comparison between the modeling and experimental data is presented in Figures 7 and 8 for the three flames with different oxygen levels in the hot coflow (9, 6, and 3%). Only the results obtained with the detailed mechanism presented in paragraph 2 are discussed. Among the different simulations, in the figures we always refer to the model results obtained using the modified k - ϵ , the DO radiation model and the EDC model for the turbulence-chemistry interactions. Details on the EDC model can be found in ref. [12] and [26], while examples of its use to model complex situations where non-premixed and premixed conditions co-exist are presented by Albrecht et al., [27] and Tang et al. [28].

The temperature profiles are in good agreement with measurements, although the flames lift off is slightly over estimated. The temperature peaks at 120 mm are overestimated, especially in the case of 6 and 9% O_2 . A possible explanation for this discrepancy can be found in the corresponding oxygen radial profiles (Fig. 7). As already discussed, these profiles are affected by the turbulence kinetic energy conditions adopted at the coflow boundary. The value of $k=0.4 \text{ m}^2/\text{s}^2$ gives result with a good agreement for the 3% O_2 flame, while in the other cases the diffusion of oxygen is slightly overestimated. The increased availability of oxygen increases the combustion intensity and directly affects the temperature levels. Similar conclusions can be drawn by analyzing the H_2O profiles.

It is worth noting that the predicted value of CO at 120 mm (Fig. 8) is in quite good agreement with experimental measurements, while OH is over-predicted. This discrepancy was also observed by Christo and Dally [7], who used two different detailed kinetic schemes with EDC, and also by Kim et al. [10] and was attributed to the mixing with the fresh air. In order to better understand the reason of the discrepancy, scatter plots of measured instantaneous temperature, CO and OH at axial location $z = 120 \text{ mm}$ are presented in Fig. 9, against the CFD model. To compare the numerical predictions with the measurements, mean scalar profiles are expressed as a function of mean mixture fraction, which is computed using Bilger's formula [29]. As already

discussed and presented in Fig. 6, this location of the flame is critical because of the mixing with the oxygen of the fresh air. Moreover, the model predictions in this region are very sensitive to the boundary conditions adopted for the turbulent kinetic energy. Figure 9 indicates that the model is able to capture the flame instantaneous OH measurement but not the mean ones (Fig. 8). As already observed by Christo and Dally [7], this indicates a possible effect of localized extinctions and re-ignition phenomena which cannot be accounted for by the adopted EDC model.

5. The Kinetic Post Processor (KPP)

Details on the KPP can be found in refs. [12,15]. The KPP uses the temperature field obtained by the CFD computations and each computational cell is modeled using a chemical reactor. A fixed average temperature is assumed in each reactor and the rates of all the reactions involved in the kinetic scheme are evaluated. CFD results are also used to define the overall system by describing the mass balance equations of all the chemical species involved in the detailed kinetic scheme as well as providing the initial composition guess. For all the reactors, the steady mass balance of each species (ω_i) accounts for convection, diffusion and chemical reaction terms:

$$W_p \cdot \omega_{p,i}^{in} - W_p \cdot \omega_{p,i}^{out} + \sum_{n=1}^{N_F} [\vec{J}_{p,n,i} \cdot S_{p,n}] + V_p^* \cdot M_i \sum_{j=1}^{N_R} \nu_{ij} \cdot r_{p,j} = 0 \quad i = 1 \dots N_{SP}, \quad p = 1 \dots N_P \quad (1)$$

where W_p is the total convective flow pertaining to the reactor, N_{sp} the number of species, N_p the number of reactors (cells), N_F the number of faces with surface area S of the cell, N_R the number of reactions, V_p the volume of the cell, M is the molecular weight, r the reaction rate and ν_{ij} the stoichiometric coefficient of species i in reaction j . The mass diffusion term is the sum of all the contributions pertaining to the adjacent reactors and is computed in the following form:

$$\vec{J}_i = -\frac{\mu_T}{Sc_T} \cdot \nabla \omega_i \quad (2)$$

where Sc_t is the turbulent Schmidt number and μ_t the turbulent viscosity. The global Newton methods are not robust enough to solve this system simply using CFD results as a first-guess. It

is therefore convenient to approach a better estimate of the solution by iteratively solving the sequence of individual reactors with successive substitutions. Additional details on the KPP and its numerical method are reported in ref. [12].

Fig. 10 shows the predicted NO mass fraction for the three flames. As expected the maximum value of NO is located in the high temperature regions located in the tail of the flames. This region is significantly affected by mixing with fresh air from the surrounding air, and therefore cannot be considered a MILD combustion. In fact, very high levels of NO are formed. It is known [1] that mixing with fresh air from the surroundings starts to have an effect at ~ 100 mm above the jet exit plane. For this reason, figure 11 focuses on the NO formation in the region immediately downstream of the inlet where MILD combustion occurs, for the 9% O₂ case. It is worth noting that the peak NO levels in this region are very small when compared with standard diffusion flames with similar Reynolds numbers, because of dilution and low oxygen availability. In this MILD combustion region the initial NO is formed according to both NNH and N₂O mechanisms. Prompt-NO formation requires CH_i+N₂ reactions to form HCN, which is then subsequently oxidized to NO. HCN formation occurs at an axial location which is shifted downstream of the typical NNH and N₂O mechanisms (Fig. 11). This difference depends on the time required for the formation of CH_i radicals, which is based on the methane combustion mechanism, while the formation of N₂O and especially NNH is directly linked to the oxidation of H₂. Hydrogen is more reactive, therefore NNH is more rapidly formed.

Figure 12 shows the comparison between measured [1] and predicted NO at two different axial locations. The agreement is satisfactory at $z=60$ mm while NO is over-predicted at 120 mm. The underestimation of NO on the axis of symmetry (Radial distance = 0) is likely due to a difficulty in correctly representing the jet characteristics. In fact, the same deviation can be observed for CO, H₂O and temperature profiles in fig. 7. Further studies are underway to explain this behavior.

As expected and experimentally observed, the peak values of NO coincides with the position of the flame front. The absolute value is correctly represented both at 6 and 9 % O₂. The over-prediction of the NO profiles at $z=120$ mm reflects the difficulty in correctly representing the local temperature peaks. As indicated in figure 13 and also in figure 7, the temperature peak is overestimated of ~ 100 K, especially in the case of the flame with 9% O₂. Whereas, figure 13 indicates that the temperature peak at $z=60$ mm is in good agreement with experimental measurements, which resulted in good prediction of the NO_x profile although it is slightly underestimated. This observation indicates that a progress in the KPP simulations is possible only on the basis of an improved CFD simulation.

6. Conclusions

A detailed CFD study of a CH₄/H₂ MILD combustion burner (JHC) has been presented using different turbulence and radiation models. A detailed kinetic mechanism able to describe the combustion of light hydrocarbons is used in the CFD simulations using the EDC approach to model turbulent combustion. This scheme is here further validated using recent experimental data on the effect nitrogen dilution on the flame velocity of CH₄ and CH₄/H₂ mixtures.

Due to the mixing with the surrounding fresh air, the accuracy of the numerical solution is found to be highly sensitive to boundary conditions, especially turbulence quantities. The modified k- ϵ model succeeded in simulating the fuel jet fluid dynamics flame structure. CFD results were validated using experimental measurements and then post-processed using a detailed Kinetic Post Processor (KPP). The computed results were validated in terms of NO formation and the overall agreement with experimental measurements is satisfactory.

The discrepancies between measured and predicted NO profiles can be attributed to the overestimation of the temperature field at axial distances larger than ~ 100 mm. In this region the mixing with surrounding air is known to play a significant role. An important goal of the future activity will be to better describe the conditions at the boundaries to improve the CFD simulation in this region. Nevertheless, the results are encouraging and the model will be applied for the design of new advanced combustors. Of course, the reliability of KPP predictions is strongly dependent on the accuracy of the CFD simulation.

Acknowledgements

The authors gratefully acknowledge the financial support of RIELLO SpA – Burners Division.

References

1. Dally B.B., Karpetis A.N., Barlow R.S., Proceedings of the Combustion Institute 29 (1), pp. 1147-1154 (2002).
2. Tatouh T., Halter F., Mounaïm-Rousselle C., The Effect of Hydrogen Enrichment on CH₄-Air Combustion in Strong Dilution, *XXXI Meeting on Combustion*, Torino, June 17-20 (2008).
3. Wüning J.A. and Wüning J.G., *Prog. Energy Combust. Sci.* 23 12 (1997), pp. 81–94.
4. Weber R., Verlaan A.L., Orsino S. and Lallemand N., *J. Inst. Energy* 72 (1999), pp. 77–83.
5. Katsuki M., Hasegawa T., Science and technology of combustion in highly preheated air, *Proc. Comb. Inst.* 27:3135 (1998).
6. De Joannon M., Saponaro A., Cavaliere A., Zero-dimensional analysis of diluted oxidation of methane in rich conditions, *Proc. Comb. Inst.* 28(2):1639-1645 (2000)
7. Christo F.C., Dally B.B., Modeling turbulent reacting jets issuing into a hot and diluted coflow. *Combust. Flame* 142 (1-2), pp. 117-129 (2005).
8. Coelho P.J. and Peters N., Numerical simulation of a mild combustion burner, *Combust. Flame* 124(3):503-518 (2001).
9. Mancini M., Weber R., Bollettini U., Predicting NO_x emissions of a burner operated in flameless oxidation mode, *Proc. Comb. Inst.* 29 (1):1155-1162 (2002)
10. Kim S.H., Huh K.Y., Dally B., CMC modeling of turbulent nonpremixed combustion in diluted hot coflow, *Proc. Comb. Inst.* 30 (1), pp. 751-757 (2004).
11. Frassoldati A., Frigerio S., Colombo E., Inzoli F., Faravelli T., Determination of NO_x emissions from strong swirling confined flames with an integrated CFD-based procedure, *Chem. Eng. Sci.* 60, pp. 2851-2869, (2005).
12. Cuoci A., Frassoldati A., Buzzi Ferraris G., Faravelli T., Ranzi E., Ignition, Fluid Dynamics and Kinetics Aspects of Syngas Combustion, *Int. J. of Hydrogen Energy*, 32: 3486-3500 (2007)
13. Barendregt S., Risseuw I., Waterreus F., Frassoldati A., Buzzi Ferraris G., Faravelli T., Ranzi E., Li X.J., Patel A.R., Combustion modeling of ethylene furnaces applying ultra low NO_x LSV™ burners, *AIChE Spring Annual Meeting* (2006).
14. Frassoldati A., Cuoci A., Faravelli T., Ranzi E., Colantuoni S., Di Martino P., Cinque G., Experimental and modeling study of a low NO_x combustor for aero-engine turbofan, *Combust. Sci. and Tech.*, 181: 1–13, (2009).
15. Frassoldati, A., Cuoci, A., Faravelli, T., Ranzi, E., Astesiano, D., Valenza, M., Sharma, P., Experimental and modelling study of low-NO_x industrial burners, *Metallurgical Plant and Technology International* 31 (6), pp. 44-46 (2008).

16. Ranzi, E., Sogaro, A., Gaffuri, P., Pennati, G., Faravelli, T., Wide range modeling study of methane oxidation, *Combust. Sci. and Tech*, 96:4-6, 279-325 (1994)
17. Faravelli, T., Frassoldati, A., Ranzi, E., Kinetic Modeling of Mutual Interactions in NO-Hydrocarbon Low Temperature Oxidation, *Combust. Flame*, 132/1-2 pp 188 - 207 (2003).
18. Ranzi, E., Frassoldati, A., Granata, S., Faravelli, T., Wide-Range Kinetic Modeling Study of the Pyrolysis, Partial Oxidation, and Combustion of Heavy n-Alkanes, *Ind. Eng. Chem. Res.* (2005) 44(14), 5170-5183.
19. Frassoldati, A., Faravelli, T., and E. Ranzi Kinetic Modeling of Mutual Interactions in NO-Hydrocarbon High Temperature Oxidation, *Combust. Flame* 135, pp. 97-112, (2003)
20. Frassoldati, A., Faravelli, T., Ranzi, E., A wide range modelling study of NO_x formation and nitrogen chemistry in hydrogen combustion, *Int. J. of Hydrogen Energy* 31(15):2310-2328 (2005).
21. Frassoldati, A., Faravelli, T., Ranzi, E., Ignition, Combustion and Flame Structure of Carbon Monoxide/Hydrogen Mixtures. Note 1: Detailed Kinetic Modeling of Syngas Combustion also in Presence of Nitrogen Compounds, *Int. J. of Hydrogen Energy* 32: 3471-3485 (2007)
22. Shimizu, T., Williams, F. A. and Frassoldati, A., Concentrations of Nitric Oxide in Laminar Counterflow Methane/Air Diffusion Flames, *Journal of Propulsion and Power* 21(6):1019-1028, November-December (2005).
23. Dally, B.B., Fletcher, D.F. and Masri, A.R., *Combust. Theory Modeling*, 2:193 (1998).
24. FLUENT6.3.26, User's Guide.
25. Barlow, R.S., Karpetis, A.N., Frank, J.H., Chen, J.-Y., *Comb. Flame* 127, 2102–2118 (2001)
26. Magnussen, B. F, On the structure of turbulence and a generalized Eddy dissipation concept for chemical reactions in turbulent flows. 19th AIAA aerospace science meeting, St. Louis, Missouri, 1981.
27. Albrecht, B.A., Zahirovic, S., Bastiaans, R.J.M., van Oijen, J.A., de Goey, L.P.H., A premixed flamelet-PDF model for biomass combustion in a grate furnace, *Energy & Fuels* 2008, 22, 1570–1580.
28. Tang, Q., Denison, M., Adams, B., and Brown, D., Towards comprehensive computational fluid dynamics modeling of pyrolysis furnaces with next generation low-NO_x burners using finite-rate chemistry, *Proc. Comb. Inst.* 32 (2009) 2649–2657
29. R.W. Bilger, *Combust. Flame* 80 135–149 (1990)

List of Figure Captions

Figure 1. Effect of nitrogen dilution on the laminar flame speed of methane-air stoichiometric flames. The effect of hydrogen addition is also presented. Comparison between prediction (lines) and measurements [2] (symbols).

Figure 2. 2D view of the computational domain and boundary conditions. Boundary conditions are indicated in the figure. Walls are assumed adiabatic.

Figure 3. Temperature field [K]: effect of the oxygen content in the oxidizer stream [mass fractions 3, 6, 9 %].

Figure 4. Axial profiles of mixture fraction along the axis of symmetry for different turbulence models (9% O₂ flame)

Figure 5. Effect of the boundary condition adopted for the turbulent kinetic energy of the coflow stream (3 % O₂ flame)

Figure 6. O₂ radial profiles [1] at two axial locations ($z=30$ and 120 mm). Effect of the boundary condition adopted for the turbulent kinetic energy of the coflow stream (3 % O₂ flame).

Figure 7. Radial profiles of Temperature [K], H₂O and O₂ [1] at two axial locations ($z=30$ and 120 mm) for the three flames.

Figure 8. Radial profiles of CO and OH [1] at two axial locations ($z=30$ and 120 mm) for the three flames.

Figure 9. Comparison between measurements (instantaneous, symbols [1]) and model predictions (line). Temperature [K], OH and CO profiles (in the mixture fraction space) for the 9, 6, and 3% O₂ flames at $z = 120$ mm.

Figure 10. NO field [mass fraction]: effect of the oxygen content in the oxidizer stream [3, 6, 9 %].

Figure 11. N-containing species [mass fraction] for the 9 % O₂ flame: detail of the MILD combustion region ($z < 150$ mm).

Figure 12. Radial profiles of NO at two axial locations ($z = 60$ and 120 mm) for the 6 and 9 % O₂ flames. Comparison between experimental measurements [1] and model (KPP) predictions.

Figure 13. Comparison between measurements (symbols [7]) and model predictions (line). Temperature [K] profiles (in the mixture fraction space) for the 9 % O₂ flame, at $z = 60$ and 120 mm.

Figures

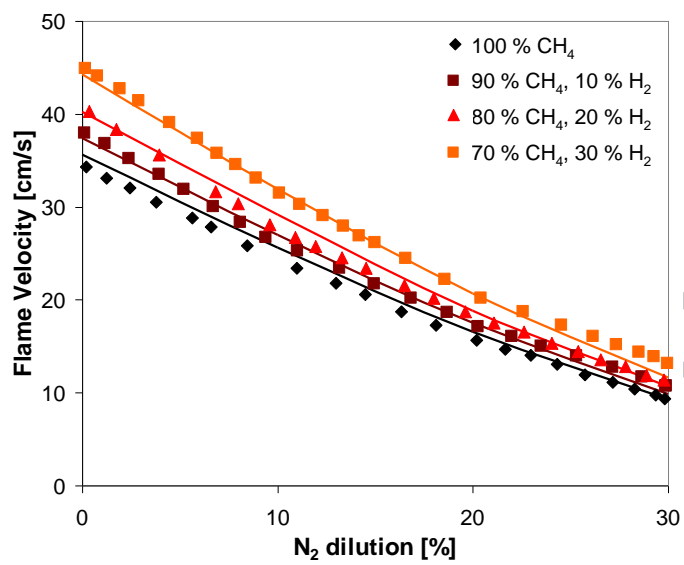


Fig. 1.

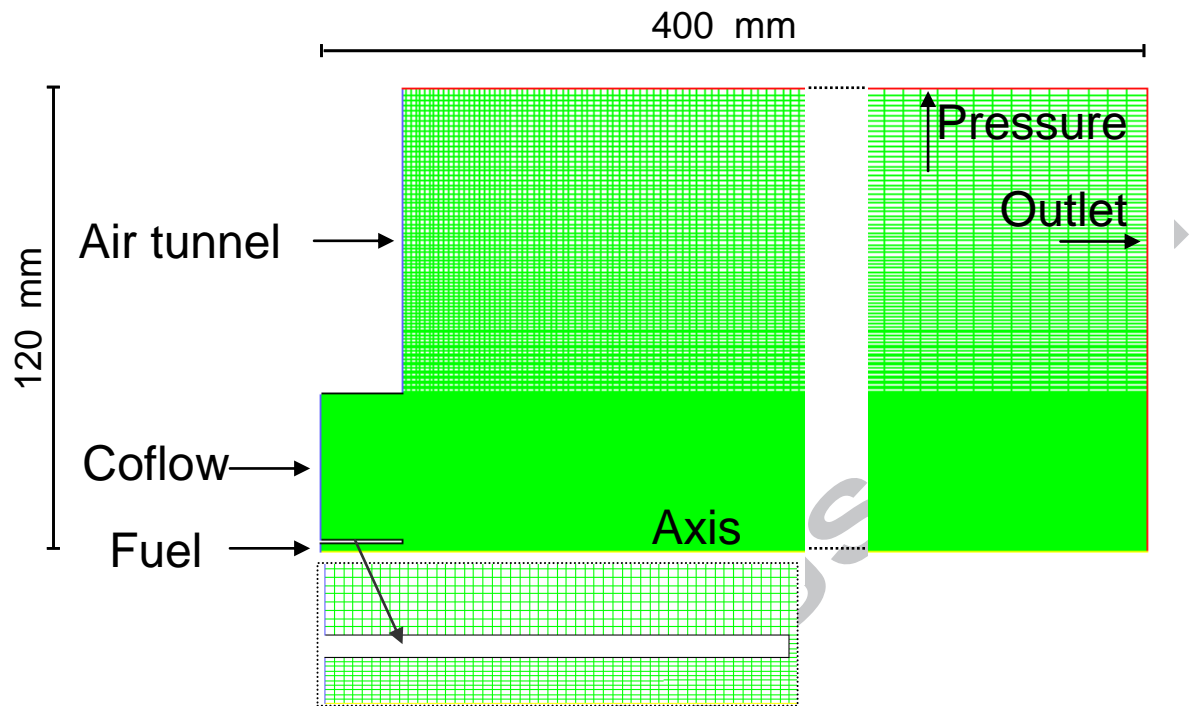


Fig. 2.

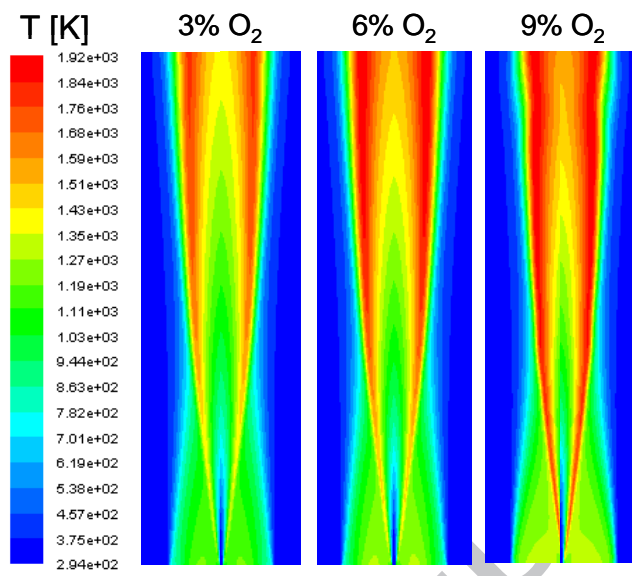


Fig. 3.

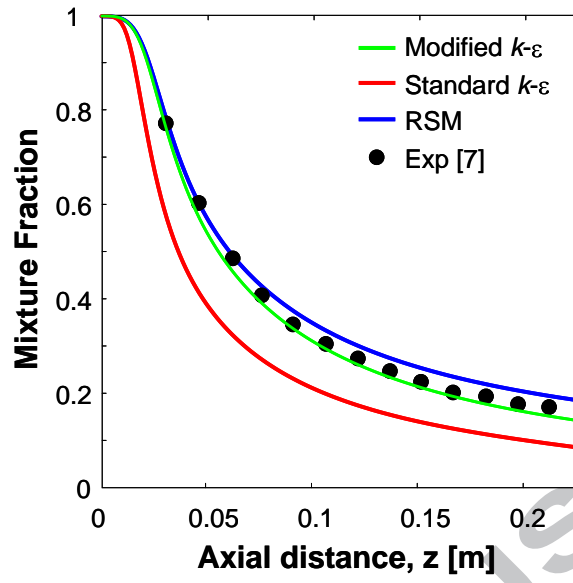


Fig. 4.

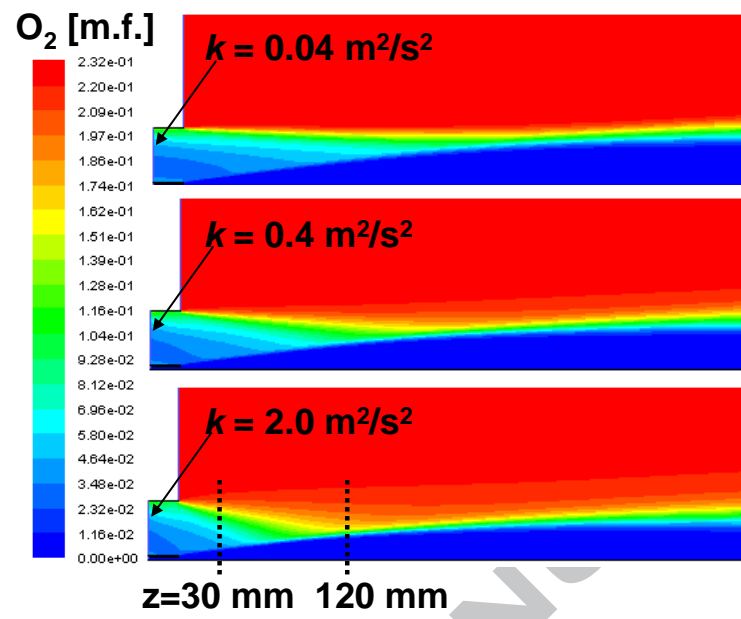


Fig. 5.

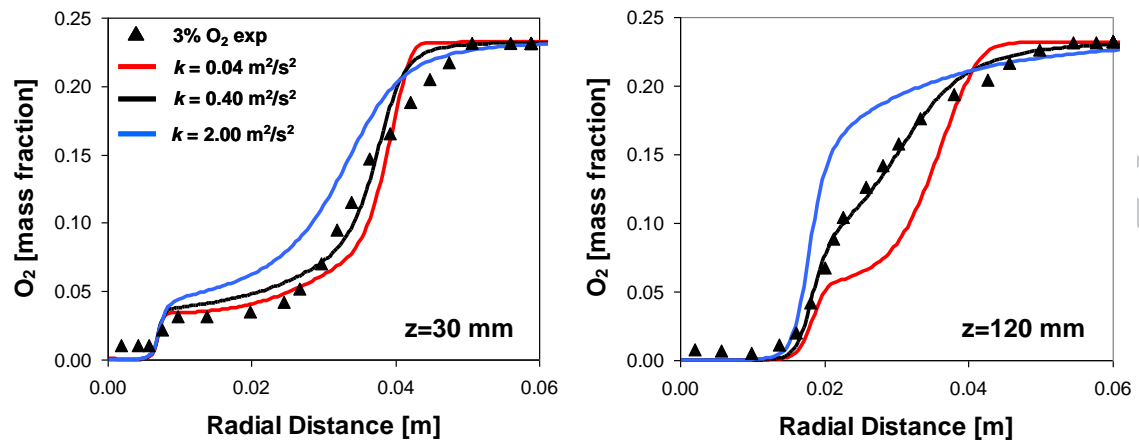


Fig. 6.

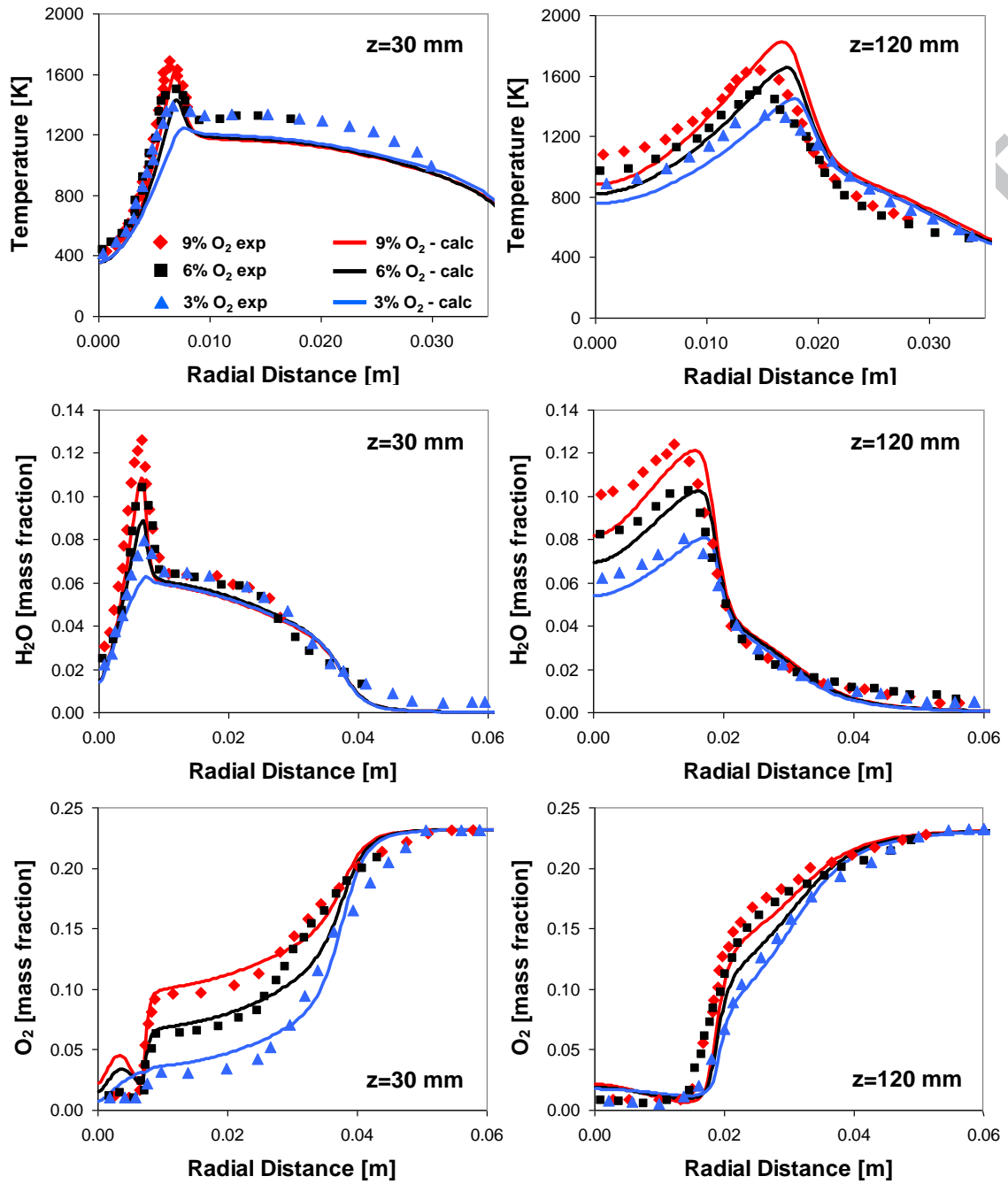


Fig. 7.

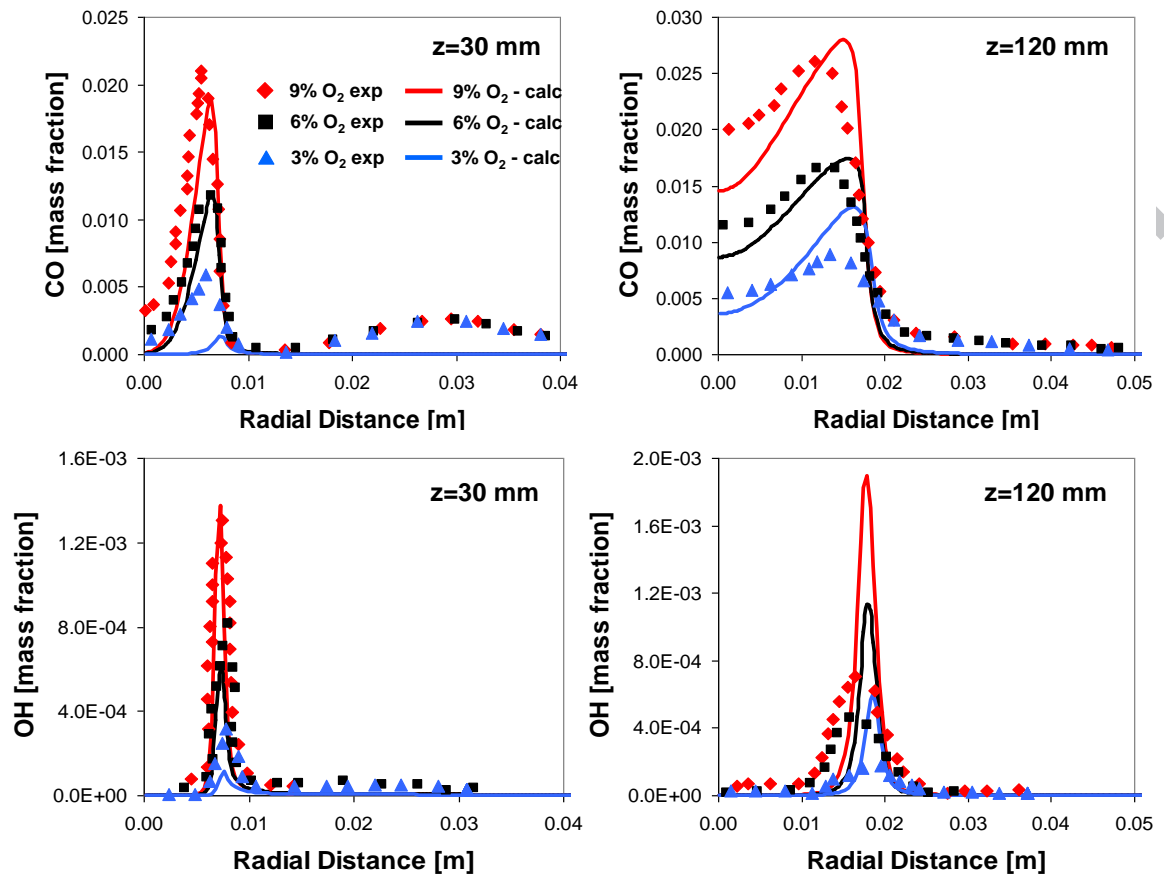


Fig. 8.

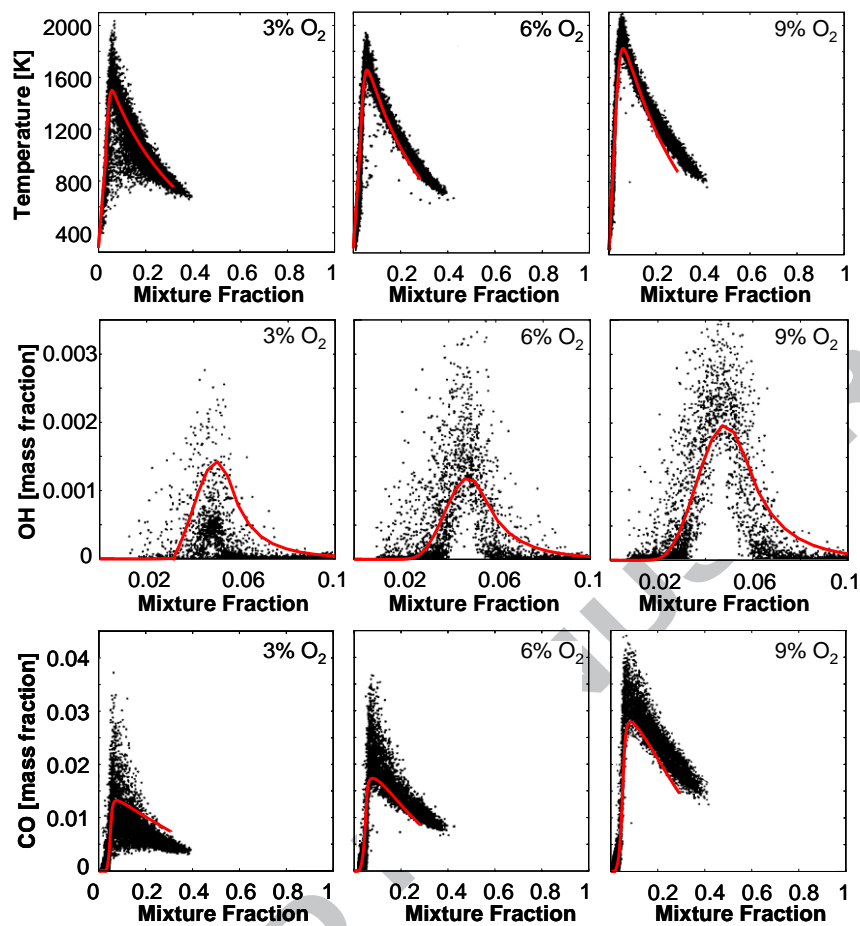


Fig. 9.

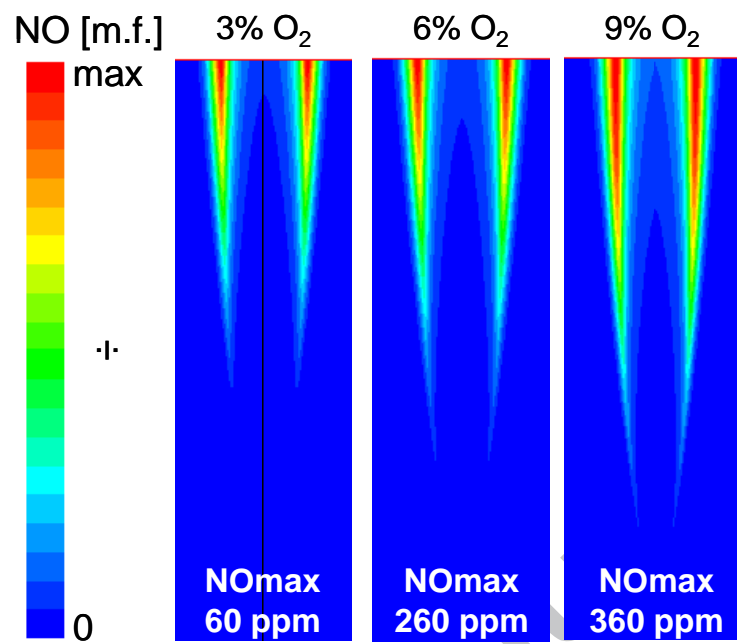


Fig. 10.

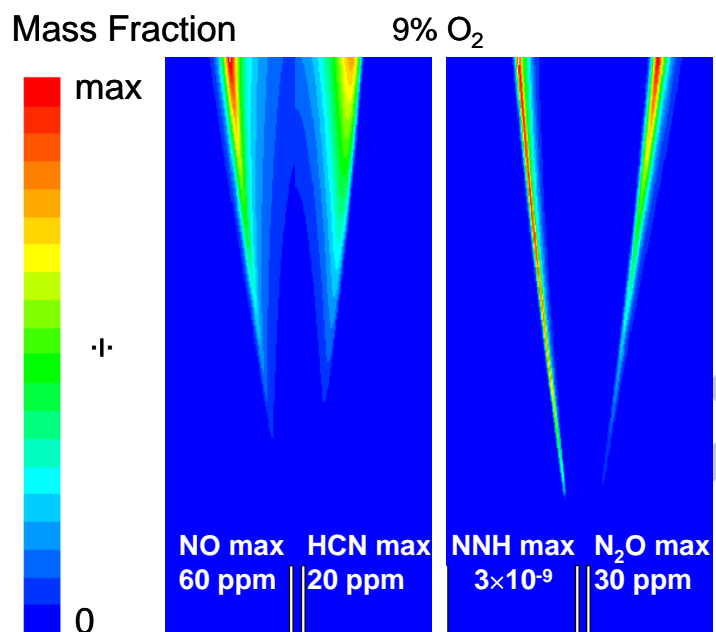


Fig. 11.

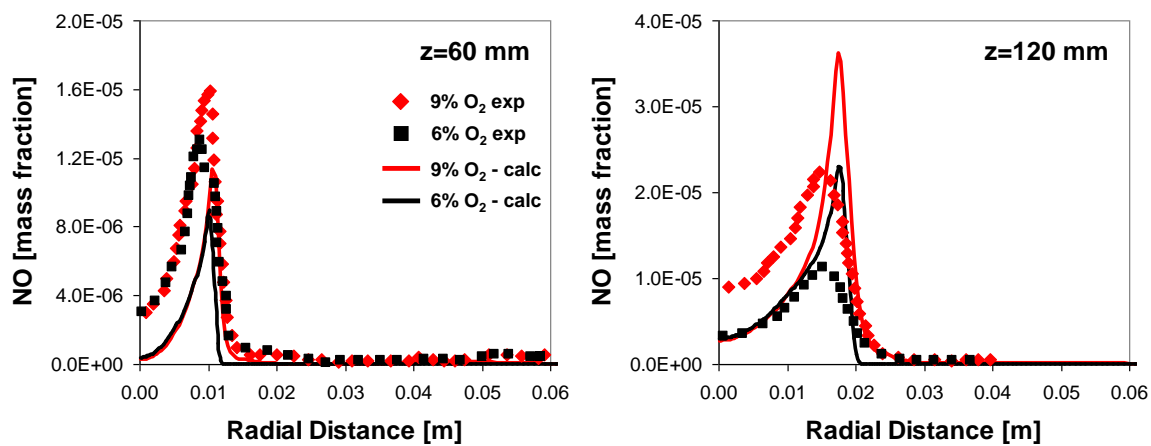


Fig. 12.

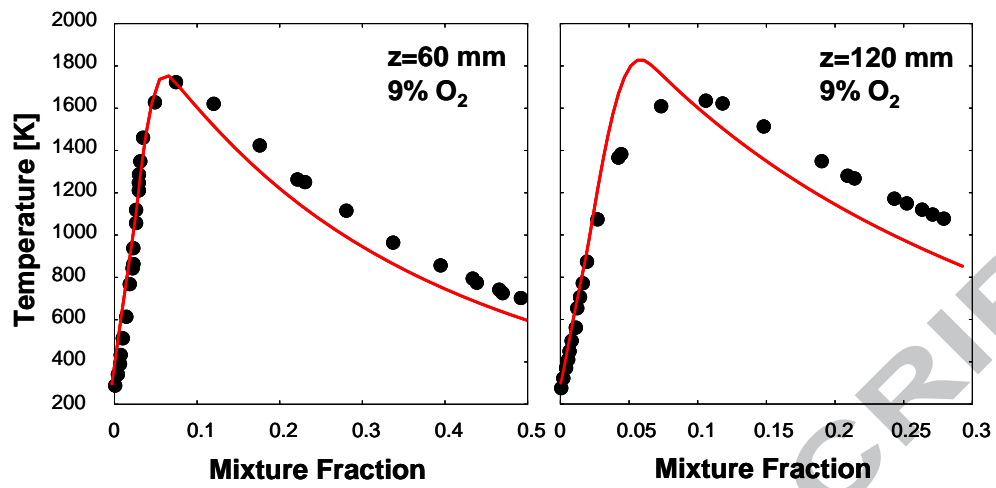


Fig. 13.

Tables

Table 1: Boundary conditions

	Central Jet	Coflow	Tunnel
Temperature	305 K	1300 K	294 K
Inlet velocity	58.74 m/s	3.2 m/s	3.3 m/s
Composition [mass fraction]	0.88 CH ₄ 0.11 H ₂	Measured Profiles [1]	0.232 O ₂ 0.768 N ₂